Limnol. Oceanogr., 43(5), 1998, 870–876

Scattering and attenuation properties of *Emiliania huxleyi* cells and their detached coccoliths

Kenneth J. Voss
Department of Physics, University of Miami, Coral Gables, Florida 33124

William M. Balch
Bigelow Laboratory for Ocean Sciences, McKown Point, West Boothbay Harbor, Maine 04575

Katherine A. Kilpatrick
Division of Meteorology and Physical Oceanography, Rosenstiel School for Marine and Atmospheric Science, University of Miami, 4600 Rickenbacker Causeway, Miami, Florida 33149

Abstract

Measurements of the spectral scattering and attenuation properties of coccolithophores (*Emiliania huxleyi*; clone 88E) and their associated coccoliths were made for three growth phases as well as for acidified cultures. These measurements allow a clean separation and determination of the optical effects of the various components. The beam attenuation cross sections (m^2 $particle^{-1}$) were found to be 8.4E-12, 2.6E-10, and 4.9E-11 for coccoliths, plated cells, and naked cells, respectively, at 440 nm. The spectral dependence of these factors followed a power law dependence, with a wavelength exponent of −1.9, 0.42, and −0.52 for the coccoliths, plated cells, and naked cells. The volume scattering functions for all appeared similar; however, the backscattering cross sections (m^2 $particle^{-1}$) at 456 nm were 1.4E-13, 6.7E-12, and 9.9E-13, respectively. The wavelength dependence of this parameter also followed a power law and was −1.4, −1.2, and −1.0. Overall, these results show that optical properties of a coccolithophore bloom are sensitive to the coccolith : cell ratio and can vary between and within blooms.

The coccolithophore *Emiliania huxleyi* (Lohm.) Hay and Moler, strain 88E, is a ubiquitous species in the worlds' oceans, common in both bloom and nonbloom conditions (Green and Leadbeater 1994). It has a major effect on carbon flux in the oceanic system and, through effects on the optical properties of the water column, on remote sensing. *E. huxleyi* produces calcite coccoliths that cover the cell, increasing its effective index of refraction and changing its scattering properties. It can also release these coccoliths, adding free coccoliths to the water column and, when growing more, continue to release these until the optical effects of free coccoliths in the water column become significant. Finally, as with other phytoplankton, the cells themselves, quite apart from coccoliths, will add to the water column attenuation and scattering. To determine the relative optical effect of free coccoliths and plated or naked cells, these optical properties must be determined separately in some manner. In field experiments, optical effects of calcite coccoliths have been isolated by bubbling with CO_2 or by adding acid (Kilpatrick et al. 1994). However, in this process both coccoliths attached to cells and detached in the medium are dissolved, and thus separating the effects of attached and detached coccoliths is difficult. Laboratory cultures of *E. huxleyi* can be grown, which allow easier manipulation, cleaner interpretation, and separation of the optical signatures of the various components of this species. The measurements reported in this paper are the first separate determinations of the optical properties of spectral backscattering, b_b, and spectral beam attenuation, c, for coccoliths, plated cells, and naked cells.

Acknowledgments

This work was supported by the Ocean Optics program of the Office of Naval Research under contract N00014-95-10309 (K.V.). W.M.P. was supported by the ONR Ocean Optics program (N00014-91-J-1048), NASA (NAS5-31363 and NAGW 2426), and NSF (OCE90-22227 and OCE 95-96167). We also thank Al Chapin for his help in making these measurements. Finally, we acknowledge the helpful comments of Annick Bricaud and an anonymous reviewer on earlier drafts of this manuscript.

Methods

Experimental design—In this experiment, volume scattering and attenuation were measured for cultures of *E. huxleyi* in three distinct growth phases. We also measured these optical parameters in acidified samples of the same cultures, which allowed resolution of the scattering and attenuation properties of pure suspensions of naked (unplated) cells.

In the first growth phase, cells were in stationary growth (henceforth referred to as stationary phase cells). In this phase the cells were predominately (95%) naked and virtually all coccoliths detached. When this sample was acidified the free coccoliths dissolved. Many studies have shown that optical properties such as b_b of the cells are not significantly altered during the acidification process (Balch et al. 1992, 1996*a*,*b*; Balch and Kilpatrick 1996). In the former reference, naked stationary phase cells were examined in a flow cytometer for 90° light scattering and forward-angle light scattering. Both optical properties were similar for untreated and acidified cells (*see* Balch et al. 1992). In the latter two references, volume scattering of field phytoplankton assemblages were examined before and after acidification. In regions where coccolithophores were absent, but diatoms,

dinoflagellates, and other algal classes were present, there was no change in the volume scattering after acidification (which indicates that the volume scattering functions were unaffected by acidification for a broad range of phytoplankton classes, not only Pyrmnesiophytes; *see* Balch et al. 1996*a*). As such, measurement of attenuation or scattering before and after acidification allowed the distinct determination of the optical signatures of unplated cells combined with free coccoliths, unplated cells separately, and, by difference, free coccoliths.

In the second experiment, a culture was used that was in log phase growth (henceforth referred to as log). In this case, most of the cells were plated (80%) and there were also free coccoliths. Optical measurement of the total sample then yielded a combination of plated cells, free coccoliths, and a few naked cells. The acidified sample allowed measurement of the optical properties of unplated cells. Hence, the optical properties of particle types could be resolved with these two samples in their two phases (log and stationary, acidified and nonacidified).

In a third independent sample, an older culture (where 50% of the cells had lost their coccoliths) was measured (referred to as senescent). In this case only scattering measurements were performed. In this sample the values derived from the other two growth phases were combined with cell and coccolith count information to find an estimate of the relevant optical properties, and these modeled values were compared with the values obtained by direct measurement.

Cultures—Three cultures of *E. huxleyi* (clone 88e) were grown in 10 liters of K media (Keller et al. 1987). Cultures were grown in an incubator at 19°C and a 12 : 12 L/D cycle at a PAR (photosynthetically available radiation) illumination of 51 μEinst m^{-2} s^{-1}. Cell and coccolith counts were made daily to follow the growth of the culture and extent of platedness. Aliquots of the culture were removed for optical measurements when the cells were in log, stationary, and senescent growth phases. Cell sizes (diameters) were previously measured to be 6.4 μm for cells with coccoliths and 5.2 μm for cells without coccoliths. The free coccoliths were ~3 μm in length and 2.4 μm in width (Fritz 1997). All measurements were performed at the same time each day to avoid possible problems with diel variability.

Microscope counts—Cells and free coccoliths were counted in a Palmer Maloney chamber using an Olympus BH-2 epifluorescence microscope with polarization optics. Cells were examined under both polarization and epifluorescence to determine the ratio of plated and naked cells in culture. The free coccoliths in solution were counted under polarization only. Microscopic particle counts were made daily on the original cultures and during the optical experiments after each addition of culture to the experimental tank.

Tank preparation—A blackened 210-liter drum was filled with fresh seawater taken from Bear Cut (off the RSMAS, Univ. Miami dock) and filtered overnight by recirculating the water through a 0.2-μm pore size Gelman pleated filter cartridge attached to a Mini-Giant submersible pump. The filter cartridge was removed before each experiment and the Mini-Giant remained in the drum to recirculate the seawater during measurements. The temperature in the drum was maintained at 19°C by a cooling coil made from tygon tubing that was attached to a recirculating water bath chiller.

Optical measurements—Spectral attenuation of the stationary and log phase cultures were made with the Vislab spectral transmissometer (VLST) (Petzold and Austin 1968). These measurements were done at 5 wavelengths: 440, 490, 520, 550, and 670 nm. Light scattering measurements were done with the general angle scattering meter (GASM) (Petzold 1972) at 6 wavelengths: 440, 490, 520, 550, 610, and 670 nm. The volume scattering function (VSF) was measured with this instrument at every degree between 10 and 170° from the incident beam. Light scattering was also measured using a Brice Phoenix (BP) scattering photometer at three angles (45, 90, and 135°) and at two wavelengths (436 and 546 nm). The VLST and GASM are designed to be in situ devices, and hence they require a large enough sample to immerse the instrument. This immersion was done by placing the instruments in the tank of 0.2-μm filtered seawater and sequentially adding culture aliquots. The BP measures a much smaller sample (beam size of 4 × 15 mm), which allowed much more sample manipulation (e.g. acidification).

The procedure followed for each instrument was as follows. GASM and VLST were placed in the tank filled with filtered seawater. The spectral attenuation, c, and VSF of the background seawater were measured and a sample was removed for the BP measurement. The BP measured the VSF for this sample, and the sample was acidified by adding 6.4 ml of 1.2% glacial acetic acid per liter seawater to the cuvette, and the VSF was measured again. There was no significant difference between the measured VSF for the acidified and nonacidified cases in this background seawater sample. At this point an aliquot of the culture sample was added to the water, and the barrel was stirred with an electric pump until the transmissometer readings stabilized. A subsample was removed for measurement by the BP and particle counts, and GASM and VLST measurements were then performed. Following the BP measurement, the aliquot was acidified and the VSF remeasured. *E. huxleyi* culture was added to the tank to achieve three concentrations, and measurements were performed at each stage. The maximum optical pathlength (c × geometric pathlength) measured was ~0.2, and thus multiple scattering effects were not significant. After the last culture addition the entire tank was acidified to dissolve all calcite coccoliths by adding 6.4 ml of 1.2% glacial acetic acid per liter seawater, bringing the pH to 5.5, whereupon measurements were performed both in the drum and with the BP. At this point the BP sample was acidified again to confirm that the coccoliths had been totally dissolved in the first case. This procedure was followed for each of the three cultures; however, for the senescent case, the VLST was malfunctioning, so no spectral attenuation measurements were available.

The VLST directly measures the spectral transmission over a 1-m path, $T(\lambda)$, which is converted to the spectral beam attenuation, $c(\lambda)$, by the equation

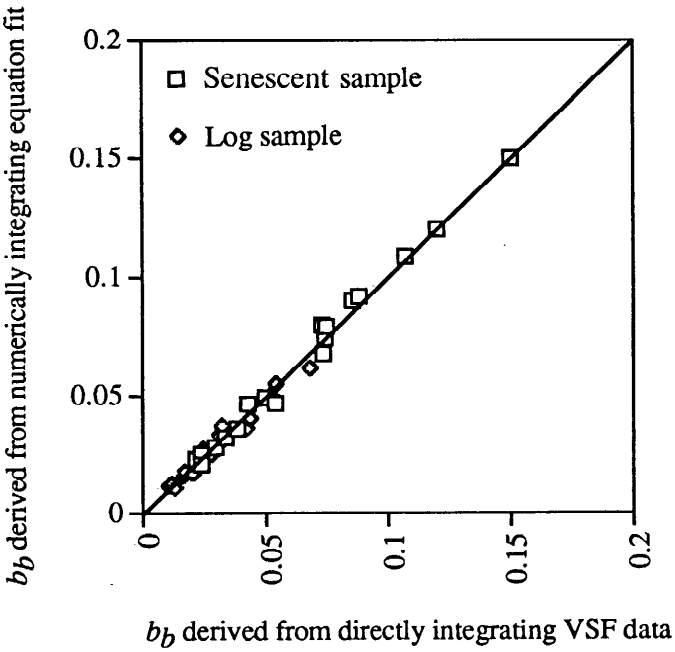

Fig. 1. Comparison of the b_b derived from the numerical fit to the Beardsley and Zaneveld (1969) equation and b_b found by directly integrating the VSF data.

$$c(\lambda) = -\ln(T(\lambda)).$$

No correction was made for the finite (~1.5°) acceptance angle of the transmissometer. This effect is estimated to cause a 10% underestimate of c (Voss and Austin 1993).

The backscattering coefficient, b_b, was calculated with the measurements of the VSF in two ways. Because the GASM measurements only extend to 170°, the data were extrapolated to 180° by assuming VSF(θ) for 170–180° is constant. The data were then integrated directly to obtain b_b through the equation.

$$b_b = 2\pi \int_{90°}^{180°} \mathrm{VSF}(\theta)\sin(\theta)\, d\theta.$$

Although more sophisticated extrapolation methods might be hypothesized, because the solid angle between 170 and 180° is such a small part of the total hemisphere and VSF(θ) is approximately flat in this region, the portion of b_b from 170 to 180° only contains 1% of the total b_b. Thus, this is probably only a ±1% error in the calculation of b_b.

For the BP, data were only obtained at three angles (45, 90, and 135°). To interpolate and extrapolate these measurements to obtain the VSF from 90 to 180°, these data were used to fit the equation (Beardsley and Zaneveld 1969; Gordon 1976)

$$\mathrm{VSF}(\theta) = \frac{f}{[1 - g\cos(\theta)]^4[1 + h\cos(\theta)]^4}.$$

Once the coefficients for this equation (f, g, and h) were determined, the equation was numerically integrated to obtain b_b. A test of this method was performed in which the GASM data were directly integrated to obtain b_b and the values of the VSF at the three angles were used to derive a b_b through the analytical fit. This was done for all the GASM measurements (Fig. 1). As can be seen, this technique works well (the SD was 6%), indicating that the b_b derived from the fitted analytic equation is accurate.

Table 1. Specific beam attenuation coefficients (standard error of the coefficients are shown in parentheses).

Wavelength (nm)	c_{cocolith}* m² lith^{-1}×10^{12}	$c_{\text{plated cell}}$* m² plated cell^{-1}×10^{10}	$c_{\text{naked cell}}$* m² naked cell^{-1} × 10^{11}
440	8.4(0.8)	2.6(0.9)	4.9(0.8)
490	6.5(0.6)	2.9(0.7)	4.6(0.6)
520	5.9(0.6)	3.0(0.6)	4.7(0.6)
550	5.3(0.6)	3.0(0.6)	4.7(0.5)
670	3.7(0.5)	3.1(0.5)	3.9(0.5)

Results

Spectral beam attenuation—As previously noted, we made two types of measurements for beam attenuation (the stationary cell case and the log case), which provided three independent variables—concentrations of naked cells, plated cells, and free coccoliths. The dependent variable is the measured beam attenuation. We also examined three concentrations of each growth phase (stationary and log), as well as the acidified sample. However, for the last sample of the log growth case, a measurement error was apparent and these data points were not used. For the beam attenuation, we have eight measurements, including associated cell and coccolith counts. A linear, multivariable, least-squares analysis (Natrella 1963) was performed, fitting the experimentally measured beam attenuation data to the equation

$$c(\lambda) = x(\lambda)X + y(\lambda)Y + z(\lambda)Z,$$

where X is the concentration of naked cells (cells m^{-3}), Y is the concentration of plated cells (cells m^{-3}), and Z is the concentration of coccoliths (coccoliths m^{-3}). The parameters determined in the fit were $x(\lambda)$, $y(\lambda)$, and $z(\lambda)$, i.e. the beam attenuation per naked cell, per plated cell, and the coccolith concentrations, respectively. In this way the relative contribution to the beam attenuation for each component could be determined. The resulting specific beam attenuation coefficients and their standard deviations for the different wavelengths are shown in Table 1 and in Fig. 2. A typical result of how well the above equation fits the data is shown in Fig. 3. This is the experimentally measured c vs. the modeled c values, using the empirically determined coefficients from the above equation. The average absolute error in the predicted c values was 7%. The cell coefficients can be compared to the measurements of Bricaud and Morel (1986), which were for naked cells (Bricaud and Morel pers. comm.). By using their table 3, the beam attenuation cross section of *E. huxleyi* can be derived as 2.44E-11 (m² cells^{-1}) (435 nm) and 2.16E-11 (m² cells^{-1}) (550 nm). These values are smaller than ours. However, the cell diameters they measured were about half of ours (not much larger than our

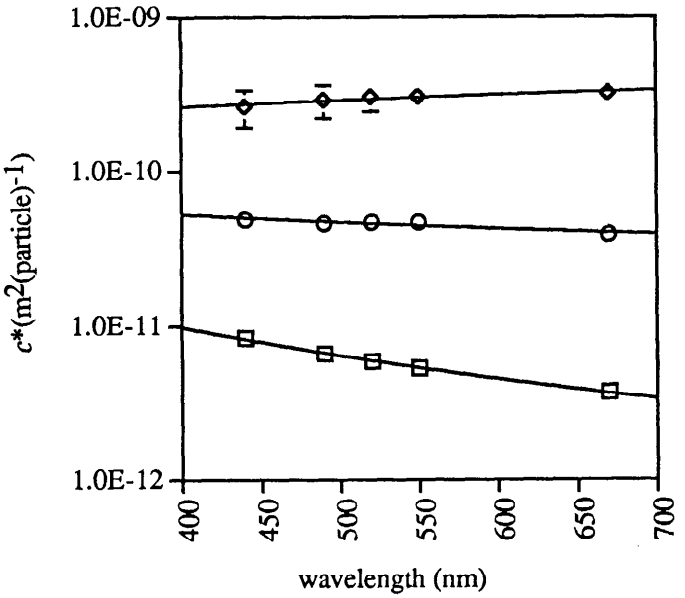

Fig. 2. Specific beam attenuation coefficients as a function of wavelength. □, coccoliths; ◇, plated cells; ○, naked cells. Also shown is the power law fit to each component (as discussed in the text). The exponent found for each component was −1.9, 0.44, and −0.52 for coccoliths, plated cells, and naked cells, respectively.

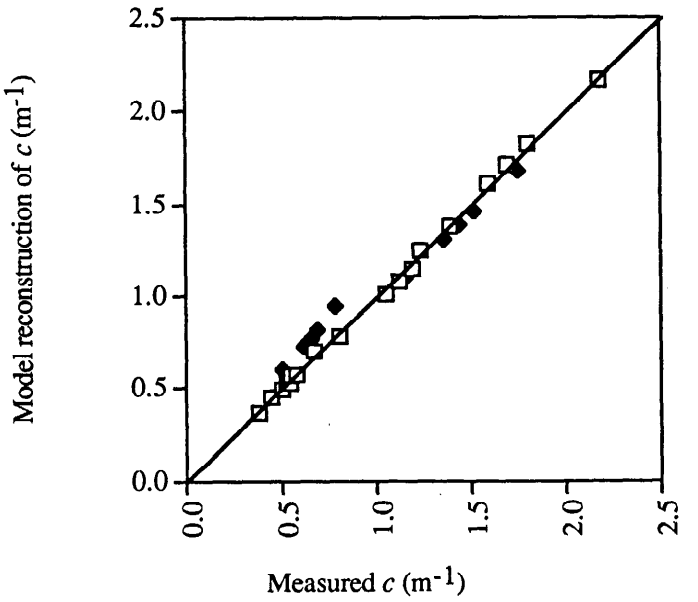

Fig. 3. The measured c compared with the reconstruction of c using cell counts and the specific attenuation coefficients of the model. □, stationary growth phase; ◆, log growth phase.

coccoliths); when normalized to cross-sectional area, these values are approximately twice our values.

Importantly, note that these data represent wavelength dependence of the factors. Each of these factors can be fit to a power law wavelength dependence (λ^{α}). The plated cell and naked cell factors are relatively spectrally flat, with wavelength exponents of −0.4 and −0.5, respectively. This agrees well with the value for naked cells derived from the Bricaud and Morel (1986) measurements (−0.5). The coccolith beam attenuation cross section is strongly wavelength dependent (a wavelength exponent of −1.9). Second, note the relative magnitude of the factors and the large increase between liths, naked cells, and plated cells.

Spectral light scattering—As in the field measurements during *E. huxleyi* blooms (Balch et al. 1991), the normalized VSF for all of the samples showed no significant spectral dependence. An example of a normalized VSF at 440 nm is shown in Fig. 4. As can be seen, there was also no marked difference in the normalized VSF between the various samples. The VSF at other wavelengths showed no difference with growth phase. Because we have no measure of the VSF between 0 and 10° it is not possible to comment on the total scattering coefficient, b. However, b_b, the backscattering coefficient, is perhaps a more important parameter because of its impact on remote sensing reflectance and diffuse attenuation.

As mentioned above, we derived b_b from both the GASM and BP measurements. The b_b measured for each sample—for the blue (440 nm for GASM, 436 for BP) and green (550 nm for GASM, 546 for BP) spectra—are shown in Fig. 5. As can be seen from these figures, the measurements with BP and with GASM agreed well for the most part, but there were some deviations.

As with the spectral c case, we performed a multiple linear fit to b_b that isolated the b_b cross sections (b_b*) for coccoliths, plated cells, and naked cells. Because b_b is an additive property, the linear, multivariable, least-squares fit took the following form:

$$b_b(\lambda) = x(\lambda)X + y(\lambda)Y + z(\lambda)Z,$$

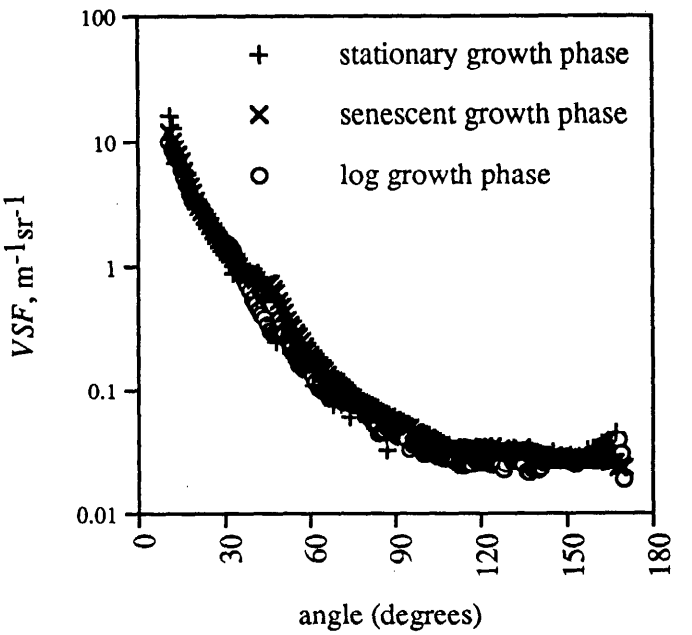

Fig. 4. Example VSF (490 nm) for each growth phase (stationary, log, and senescent).

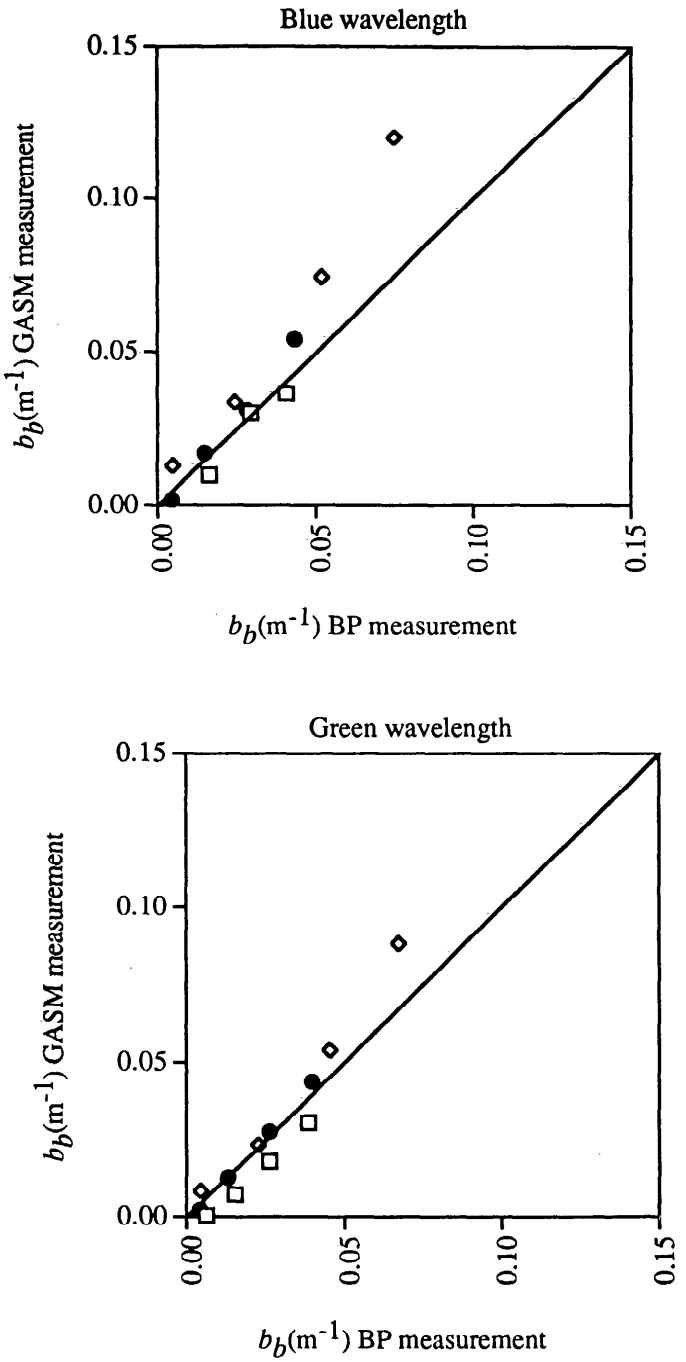

Fig. 5. Comparison of the BP measurements and GASM measurements of b_b for the same samples. □, stationary growth phase; ●, log growth phase; ◇, senescent growth phase.

where *X*, *Y*, and *Z* are the coccolith, plated cell, and naked cell concentrations. Hence, $x(\lambda)$, $y(\lambda)$, and $z(\lambda)$ represented the b_b* for coccoliths, plated cells, and naked cells. Table 2 shows the BP-GASM-derived coefficients. Fig. 6 shows the same data graphically. Note the 520 nm measurement with GASM was probably an overestimate as it was anomalously high in all the measurements with this instrument (but no reason has been found for this problem, so the measurements

Table 2. BP- and GASM-derived spectral backscattering coefficients (standard errors of the coefficients are shown in parentheses).

Wavelength (nm)	b_b*$_{\text{coccolith}}$ m^2 lith^{-1}×10^{13}	b_b*$_{\text{plated cell}}$ m^2 plated cell^{-1}×10^{12}	b_b*$_{\text{naked cell}}$ m^2 naked cell^{-1} × 10^{13}
456	1.4(0.2)	6.7(1.3)	9.9(2.3)
546	1.3(0.2)	5.8(1.2)	9.5(2.0)
440	2.1(0.2)	8.8(2.4)	1.7(1.7)
490	1.8(0.1)	9.3(1.9)	1.3(1.0)
520	2.2(0.2)	13(2.6)	1.8(1.4)
550	1.6(0.1)	6.6(1.5)	1.1(0.8)
610	1.4(0.1)	5.1(2.3)	1.7(1.2)
670	1.2(0.1)	6.5(1.3)	0.84(0.72)

are reported "as is"). First, we note that the GASM coefficients are somewhat larger than the BP coefficients (but within the standard error), particularly in the blue. The BP-derived coefficients have lower standard errors than do the GASM-derived coefficients. This is because the acidified measurements could be performed on every sample, vs. the endpoints for GASM, as discussed above. Previous work by Ahn et al. (1992) for naked *E. huxleyi* cells predicted a much smaller b_b ($Q_{bb} = 4b_b/\pi D^2$ = 2E-3 at 550 nm vs. 5E-2 in our measurements). There are two explanations for this difference. First, their method also showed a strong spectral variation in b_b, absent in our measurements, with a chlorophyll fluorescence peak evident. It is possible that the attenuation of the cells depressed their b_b measurements. In our

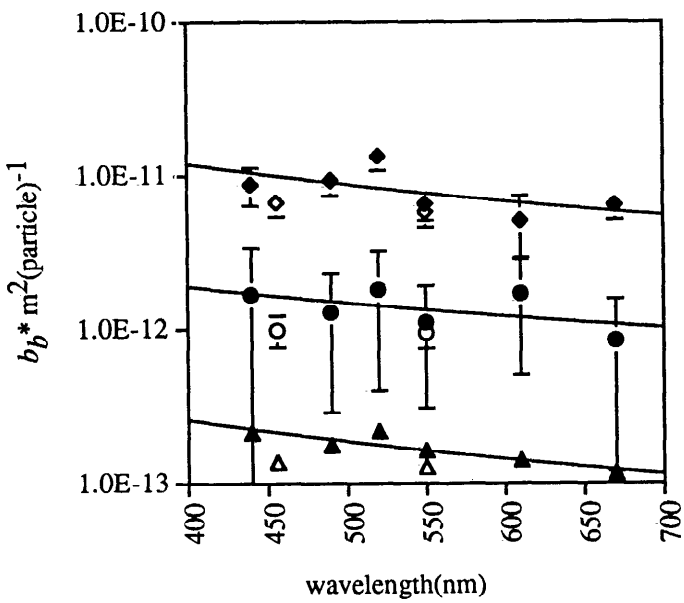

Fig. 6. Specific b_b coefficients (b_b*) as a function of wavelength for both the BP-derived and GASM-derived measurements. Open symbols are the GASM-derived coefficients; filled symbols are the BP-derived coefficients. Triangles correspond to coccoliths, diamonds to plated cells, and circles to naked cells. Also shown is the power law fit to each component (as discussed in the text). The exponent found for each component was −1.4, −1.2 and −1.0 for coccoliths, plated cells, and naked cells, respectively.

methods the cell attenuation is accounted for by a direct measurement during the measuring process. Second, the proportion of b_b due to the naked cells was quite small in almost all of our measurements and is evident in the large relative error in the derived b_b (cells m^{-2}). As shown in Table 2, the percent standard deviation for these coefficients varied between 20% (for the BP-derived coefficients) and 100% (for some of the GASM-derived coefficients), and thus we have the lowest confidence in our value for the naked coccolithophores. The wavelength dependence determined from the GASM measurements leads to a power law dependence on wavelength with exponents of −1.4, −1.2, and −1.0 for the coccolith, plated cell, and naked cell components, respectively. With this wavelength dependence, the free coccoliths may have the largest signature in remotely sensed images if differences in the visible bands are viewed.

Although in field cases it is not possible to get a separate number for the b_b* of plated cells and naked cells, some estimates of the b_b* due to coccoliths have been made. The $b_b{}^*_{\text{coccolith}}$ from the BP measurements (1.4E-13 and 1.3E-13 m^2 coccolith^{-1}) are close to the field measurements reported in Balch et al. (1991) of 1.41E-13 and 1.29E-13 m^2 coccolith^{-1} for 436 and 546 nm, respectively. Field measurements of $b_b{}^*_{\text{coccolith}}$ should be an overestimate due to neglecting the contribution of plated cells, but this does not appear to have been the case in this situation. Note that in the Balch et al. (1991) dataset, the ratio of free coccoliths to cells reached values of 400 or more; thus, the free coccoliths dominated the optical properties and the contribution by plated cells was negligible (*see* below).

Besides the wavelength dependence of these factors, it is useful to look at the absolute magnitude of the b_b*. As can be seen, the variation between components is similar to the beam attenuation coefficients. Thus, the ratio of $b_b{}^*_{\text{coccolith}}$ to $b_b{}^*_{\text{plated cell}}$ is on the order of 40.

If these b_b* coefficients are relevant for field samples, we can use them to look at the relative importance of free coccoliths to plated cells in determining the optical signature of the ocean for bloom conditions. To test these coefficients a dataset obtained during a coccolithophore bloom off of Iceland (Holligan et al. 1993; Balch et al. 1996*a,b*) was used. This dataset had counts of live cells and free coccoliths along with BP b_b measurements. Figure 7 illustrates the fit to the measurements, using the specific b_b coefficients derived above and the cell count data from the cruise, for the blue and green wavelengths of BP. The value shown in Fig. 7, b_b', is the acid-labile b_b, which is total b_b minus acidified b_b and is effectively the b_b for calcite. The coefficients used in the model were derived from the BP measurements of the laboratory cultures. The 1 : 1 line is shown along with a line representing the best fit. There seems to be an overestimate of the field data by 20%, but overall the model seems to reasonably estimate field data. The importance of this work is in showing the relative importance of the components in determining the optical properties. With counts of the separate components, we can determine the relative contribution of the plated cells and coccoliths to the total b_b in this situation. Figure 8 illustrates the portion of b_b due to plated cells vs. b_b'. b_b' should include contributions from plated cells and free liths. It appears that in this data set b_b' is

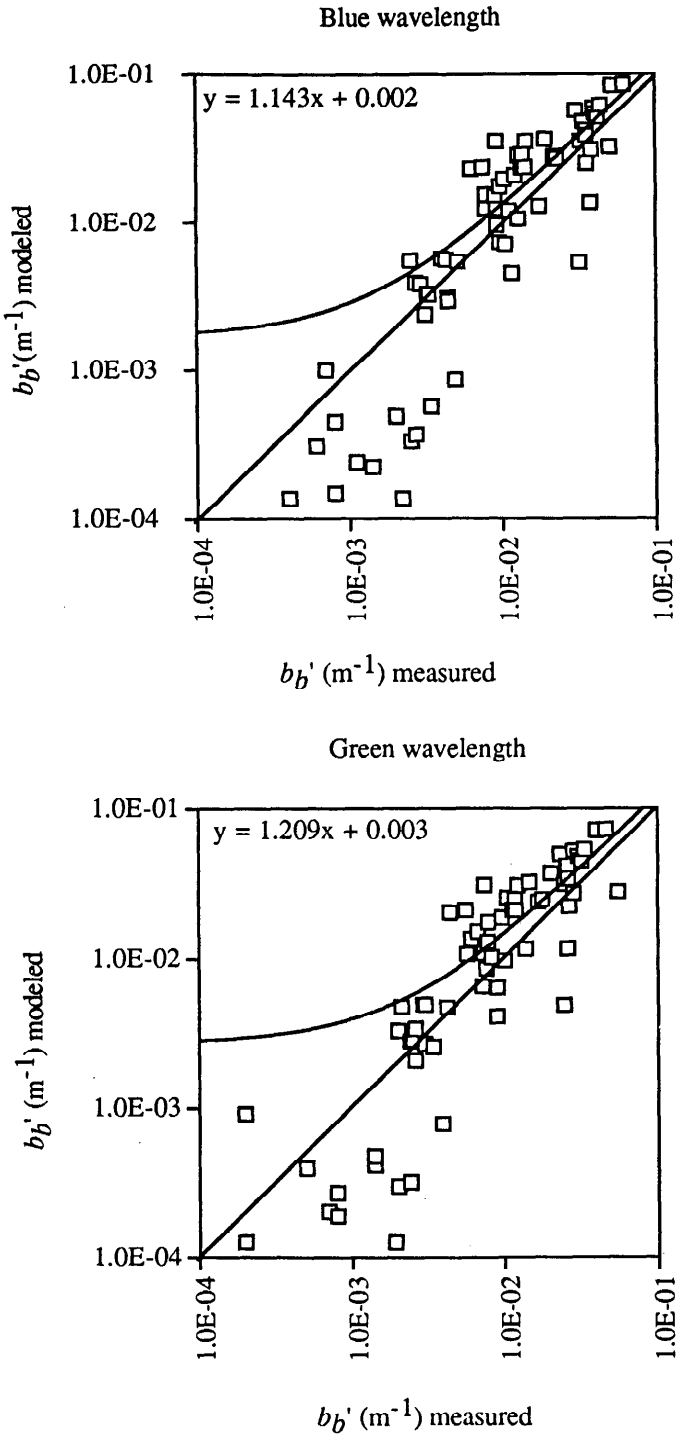

Fig. 7. Fit of empirical model to data obtained in coccolithophore bloom off of Iceland. b_b' is the acid-labile b_b, derived from the total b_b-acidified b_b for the field samples. Shown are the 1 : 1 line and a line showing the best fit between the measured and predicted values.

dominated by plated cells. If one looks at the ratio of free coccoliths to plated cells, it is clear that in this study the high b_b' cases are those dominated by cells (i.e. low detached coccolith-to-plated cell ratio). Because the ratio of free coc-

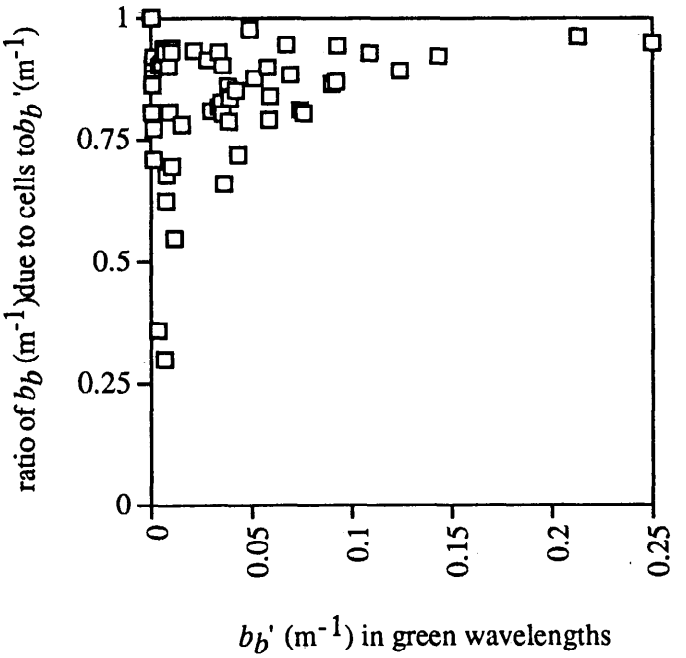

Fig. 8. Relative contribution of the b_b due to plated cells to the acid-labile b_b (b_b').

coliths to cells can vary from bloom to bloom, the importance of free coccoliths vs. cells in determining the optical properties can vary. For example, Balch et al. (1991) reported coccolith : cell ratios for blooms occurring in the Gulf of Maine for two years, 1988 and 1989. In the first case the highest free coccolith : cell ratios reported were ~50, indicating that coccoliths would have had approximately equal importance as cells in determining the backscattering. In the 1989 bloom, the coccolith : cell ratio reached values >400, and in this case the free coccoliths would have been the dominate constituent. The coccolith : cell ratio can vary within blooms and nonbloom waters, which makes this an important ratio to understand in interpretation of remote sensing reflectance.

Conclusions

We have found the specific backscattering and spectral beam attenuation coefficients for the separate components of coccoliths, plated cells, and naked cells. These show that the plated cell contribution to the optical properties can be greater than the sum of the coccoliths coating them. Thus, the optical properties of a coccolithophore bloom are sensitive to the ratio of free coccoliths to plated cells. Because the spectral variation of b_b* is different for these coefficients, the remote sensing reflectance will vary with this ratio, with the stronger spectral variation when free liths dominate the upper water column. This may be the reason that blooms with a high ratio of free liths are most evident in satellite images based on color difference techniques.

References

AHN, Y.-H., A. BRICAUD, AND A. MOREL. 1992. Light backscattering efficiency and related properties of some phytoplankters. Deep-Sea Res. **39:** 1835–1855.

BALCH, W. M., P. M. HOLLIGAN, S. G. ACKLESON, AND K. J. VOSS. 1991. Biological and optical properties of mesoscale coccolithophore blooms in the Gulf of Maine. Limnol. Oceanogr. **36:** 629–643.

———, ———, AND K. A. KILPATICK. 1992. Calcification, photosynthesis and growth of the bloom-forming coccolithophore, *Emiliania huxleyi*. Cont. Shelf Res. **12:** 1353–1374.

———, AND K. A. KILPATRICK. 1996. Calcification rates in the equatorial Pacific along 140W. Deep-Sea Res. **43:** 971–993.

———, ———, P. M. HOLLIGAN, AND C. TREES. 1996*a*. The 1991 coccolithophore bloom in the central north Atlantic 1. Optical properties and factors affecting their distribution. Limnol. Oceanogr. **41:** 1669–1683.

———, ———, ———, D. HARBOUR, AND E. FERNANDEZ. 1996*b*. The 1991 coccolithophore bloom in the central north Atlantic 2. Relating optics to coccolith concentration. Limnol. Oceanogr. **41:** 1684–1696.

BEARDSLEY, G. F., AND J. R. V. ZANEVELD. 1969. Theoretical dependence of the near-asymptotic apparent optical properties on the inherent optical properties of sea water. J. Opt. Soc. Am. **59:** 373–377.

BRICAUD, A., AND A. MOREL. 1986. Light attenuation and scattering by phytoplanktonic cells: A theoretical modeling. Appl. Optics. **25:** 571–580.

FRITZ, J. J. 1997. Growth dependence of coccolith detachment, carbon fixation, and other associated processes by the coccolithophore *Emiliania huxleyi*. Ph.D. thesis, Univ. Miami. 179 p.

GORDON, H. R. 1996. Radiative transfer in the ocean: A method of determination of absorption and scattering properties. Appl. Opt. **15:** 2611–2613.

GREEN, J. C., AND B. S. C. LEADBEATER. 1994. The haptophyte algae. Oxford science publications. The Systematics Association special vol. 51. Clarendon.

HOLLIGAN, P. M., AND OTHERS. 1993. A geochemical study of the coccolithophore *Emiliania huxleyi*. North Atlantic Global Biogeochemical Cycles **7:** 879–900.

KELLER, M. D., R. C. SELVIN, W. CLAUS, AND R. R. L. GUILLARD. 1987. Media for the culture of oceanic ultraphytoplankton. J. Phycol. **23:** 633–638.

KILPATRICK, K. A., Y. GE, W. M. BALCH, AND K. J. VOSS. 1994. A photometer for the continuous measurement of calcite-dependent light scatter in seawater. Proc. Soc. Photo-Optical Instr. **1994:** 512–521.

NATRELLA, M. G. 1963. Experimental statistics. NBS Handbook 91. U.S. Govt Printing Office.

PETZOLD, T. J. 1972. Volume scattering functions for selected ocean waters. Univ. Calif. Scripps Inst. Oceanogr. Tech. Rep. 72–78.

———, AND R. W. AUSTIN. 1968. An underwater transmissometer for ocean survey work. Univ. Calif. Scripps Inst. Oceanogr. Tech. Rep. 68-9.

VOSS, K. J., AND R. W. AUSTIN. 1993. Beam-attenuation measurement error due to small-angle scattering acceptance. J. Atmosph. Oceanic Technol. **10:** 113–121.

Received: 24 December 1996
Accepted: 22 December 1997